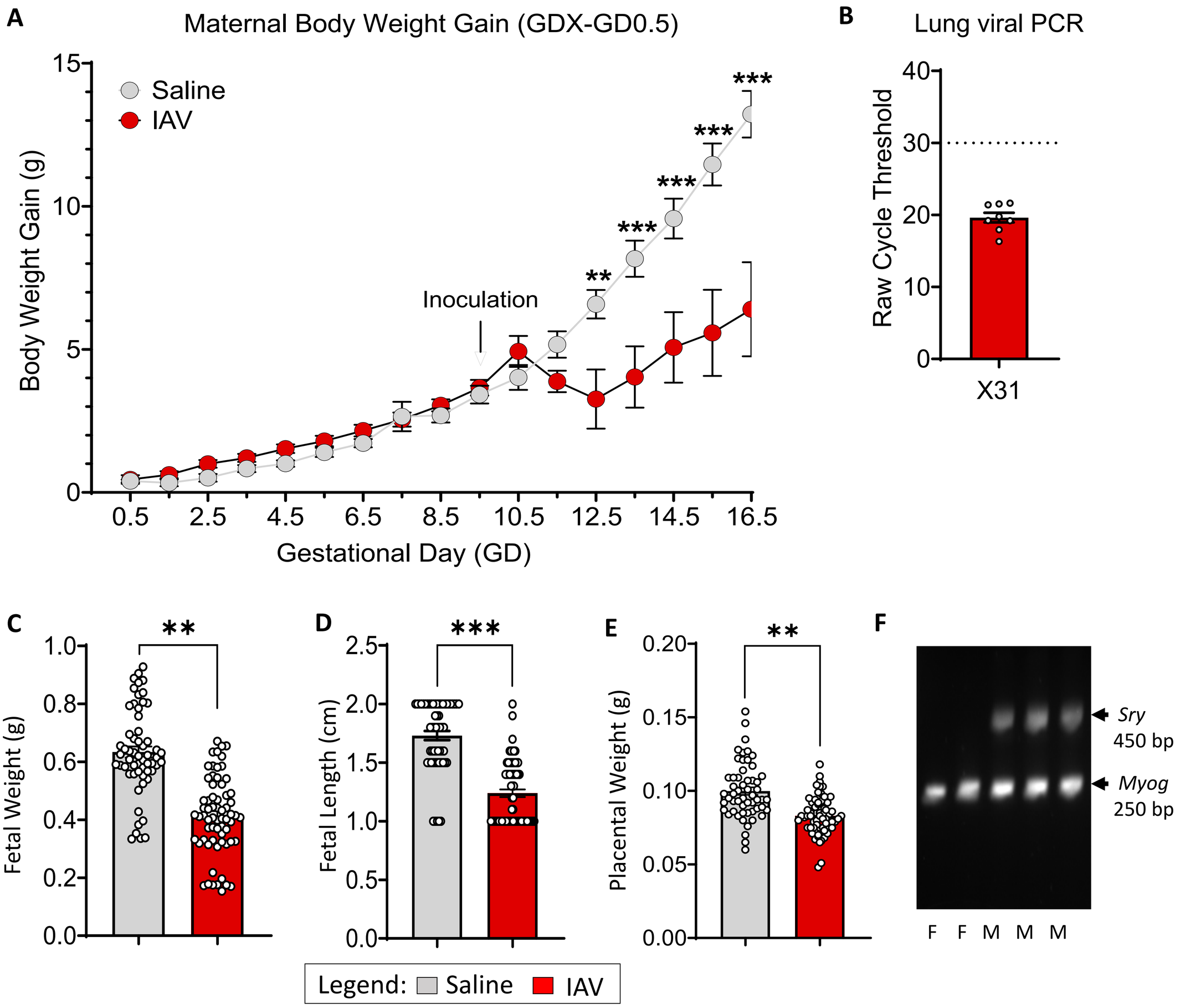

Supplementary Figure S1. Gestational IAV infection leads to systemic maternal inflammation and reduces placental and fetal weight and length. (A) Dam body weight gain trajectories (GDX–GD0.5) following IAV inoculation demonstrate a suppression in weight gain in infected dams starting at E12.5. Statistical analysis was performed using repeated-measures two-way ANOVA with Šídák's post-hoc test for multiple comparisons, revealing main effects of time ($p < 0.0001$), treatment ($p < 0.05$), and a time × treatment interaction ($p < 0.0001$). IAV-infected dams exhibited reduced body weight gain beginning at GD12.5 and persisting through GD16.5, the time of tissue collection. Data are shown as means ± SEM; n per group: Con = 8, IAV = 8. **(B)** Presence of X31 H3N2 nucleoprotein RNA in maternal lungs was confirmed by PCR using a cycle threshold of ≤ 30 cycles (dotted line) as evidence of infection. Control samples (not shown) were not below threshold. Circles represent individual dams; X31: n = 8. In panels **(C-E)**, statistical comparisons were performed using a mixed-effects model fitted with the 'nlme' package in R, where 'litter' was treated as a random effect. Circles represent individual fetuses at embryonic day (E)16.5; n per group: Saline = 58, IAV = 66; p-values = ** $p < 0.01$, *** $p < 0.001$; g = grams, cm = centimeters. Data are shown as means ± SEM. **(F)** Fetal sex was determined at E16.5 by PCR amplification of the Y-chromosome–specific *Sry* gene (450 bp), with *Myog* gene (250 bp) used as an autosomal control; bp = base pair; F = female, M = male.

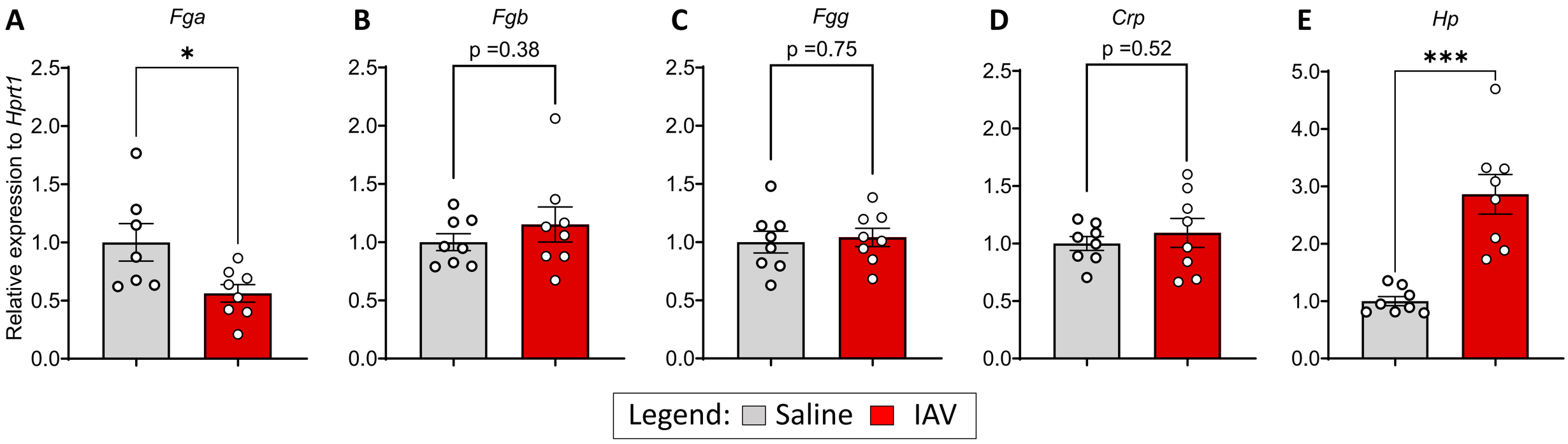

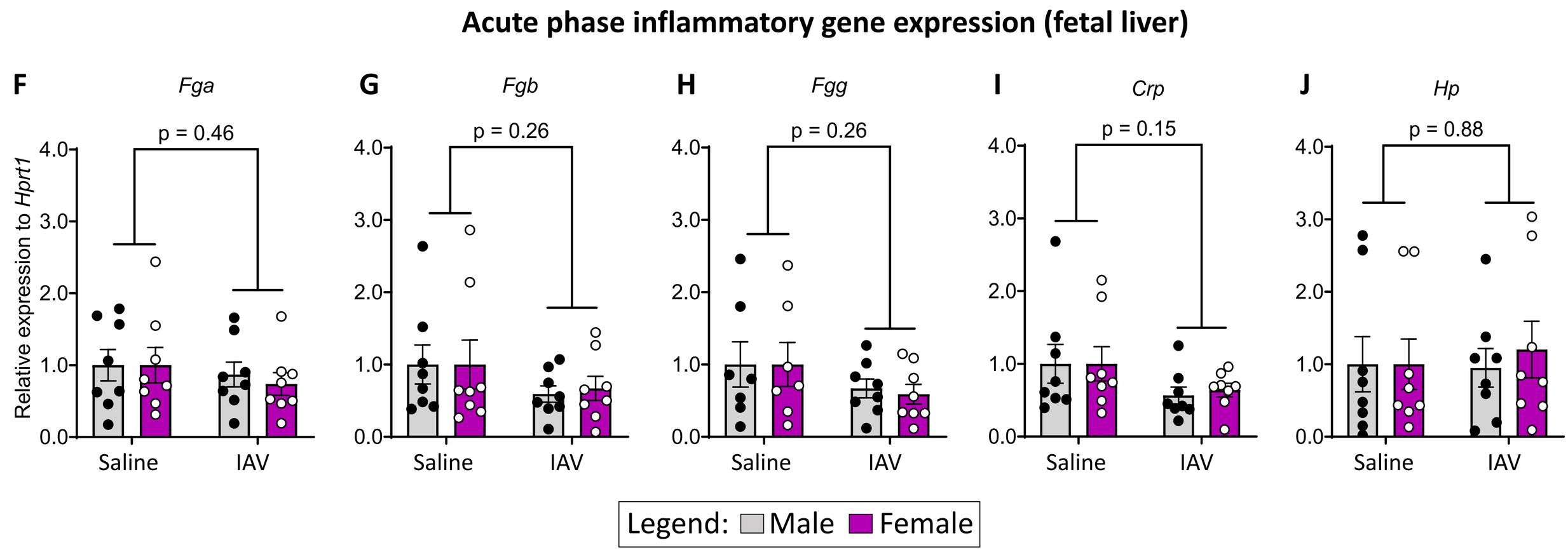

Supplementary Figure S2. Expression of acute phase inflammatory genes in maternal and fetal liver. Maternal, but not fetal, liver shows treatment-dependent changes in *Fga* and *Hp*. Panels **A–E** (Maternal liver): Panels A–D (*Fga, Fgb, Fgg*, and *Crp*) were analyzed using standard unpaired t-tests, as group variances were comparable. In **(A)**, *Fga* was significantly reduced in the IAV group compared with Saline, whereas *Fgb*, *Fgg*, and *Crp* **(B–D)** showed no treatment-related differences. In **(E)**, *Hp* exhibited unequal variances and was analyzed using Welch's t-test, revealing a significant increase in *Hp* expression in the IAV group. Data are expressed as means ± SEM; circles represent individual dams; n per group: Saline = 7-8, IAV = 8. Panels **F–J** (Fetal liver): The same acute-phase genes were analyzed in fetal liver using one male and one female fetus per litter as representative samples. Data were analyzed using linear mixed-effects models with treatment (Saline vs. IAV) and sex (male vs. female) as fixed factors and dam as a random effect to account for litter. Type III ANOVA with Satterthwaite approximation tested fixed effects. None of the genes showed significant effects of treatment, sex, or treatment × sex interaction. Data are shown as means ± SEM; circles represent individual fetuses; n/sex/group: Male = 7-8, Female = 8.

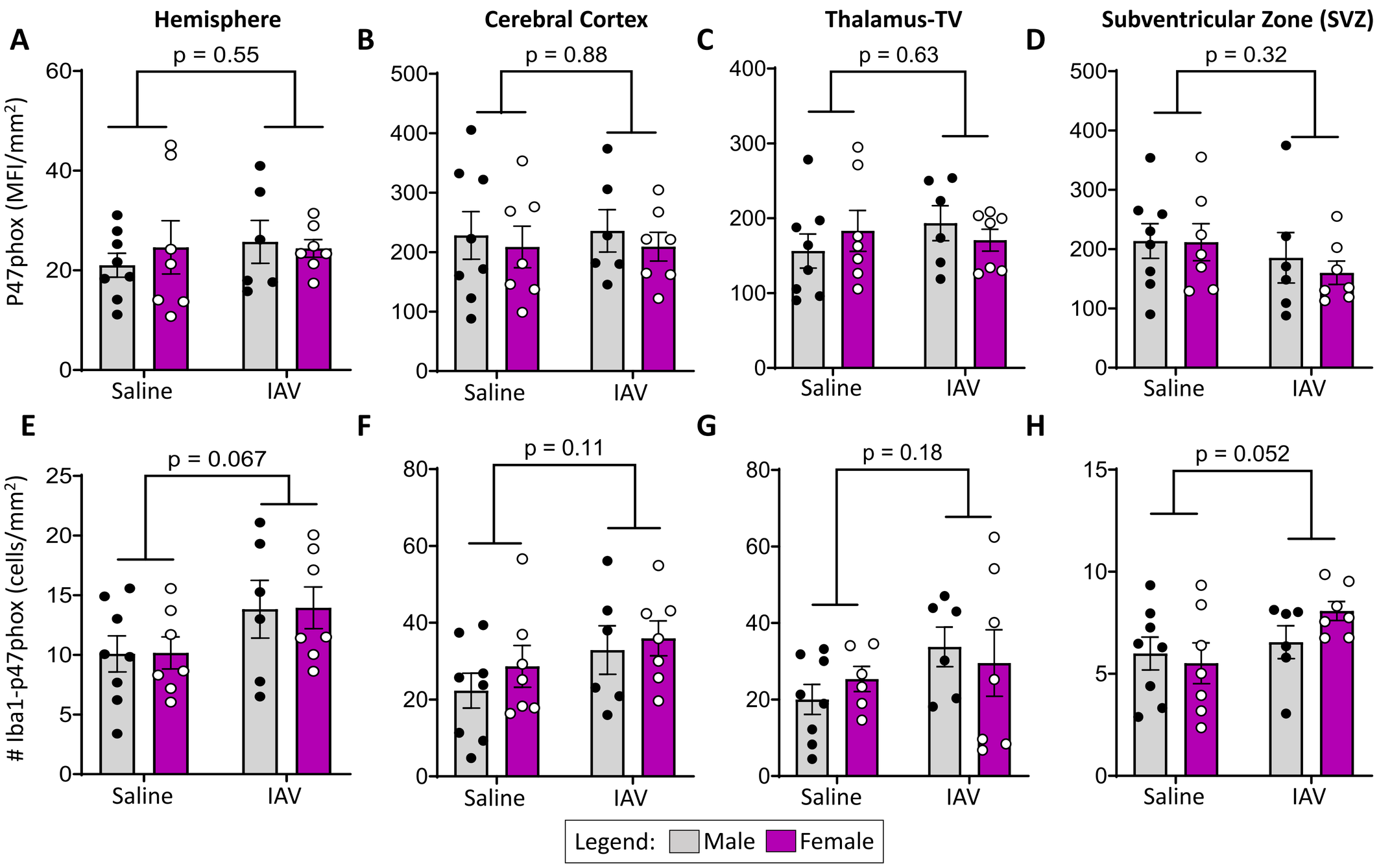

Supplementary Figure S3. Regional p47^{phox} MFI/mm² and Iba1^{+}/p47^{phox+} cell density do not show fetal sex-dependent differences. (**A-D**) Regional quantification of p47^{phox} fluorescence intensity (MFI/mm²) in the embryonic Hemisphere, Cerebral Cortex, Thalamus-TV interface, and SVZ did not reveal significant effects of fetal sex or treatment × sex interactions. (**E-H**) Similarly, Iba1^{+}/p47^{phox+} cell density did not show significant sex-dependent differences across these regions. All data were analyzed using linear mixed-effects models with treatment (saline vs IAV) and sex (male vs female) as fixed factors and dam as a random effect to account for litter effects. Type III ANOVA with Satterthwaite approximation tested fixed effects. Data are expressed as mean ± SEM; circles represent individual fetuses per dam of each group. n/sex/group: Saline: n = 7-8, IAV: n = 6-7. Thalamus-TV = thalamus-third ventricle.

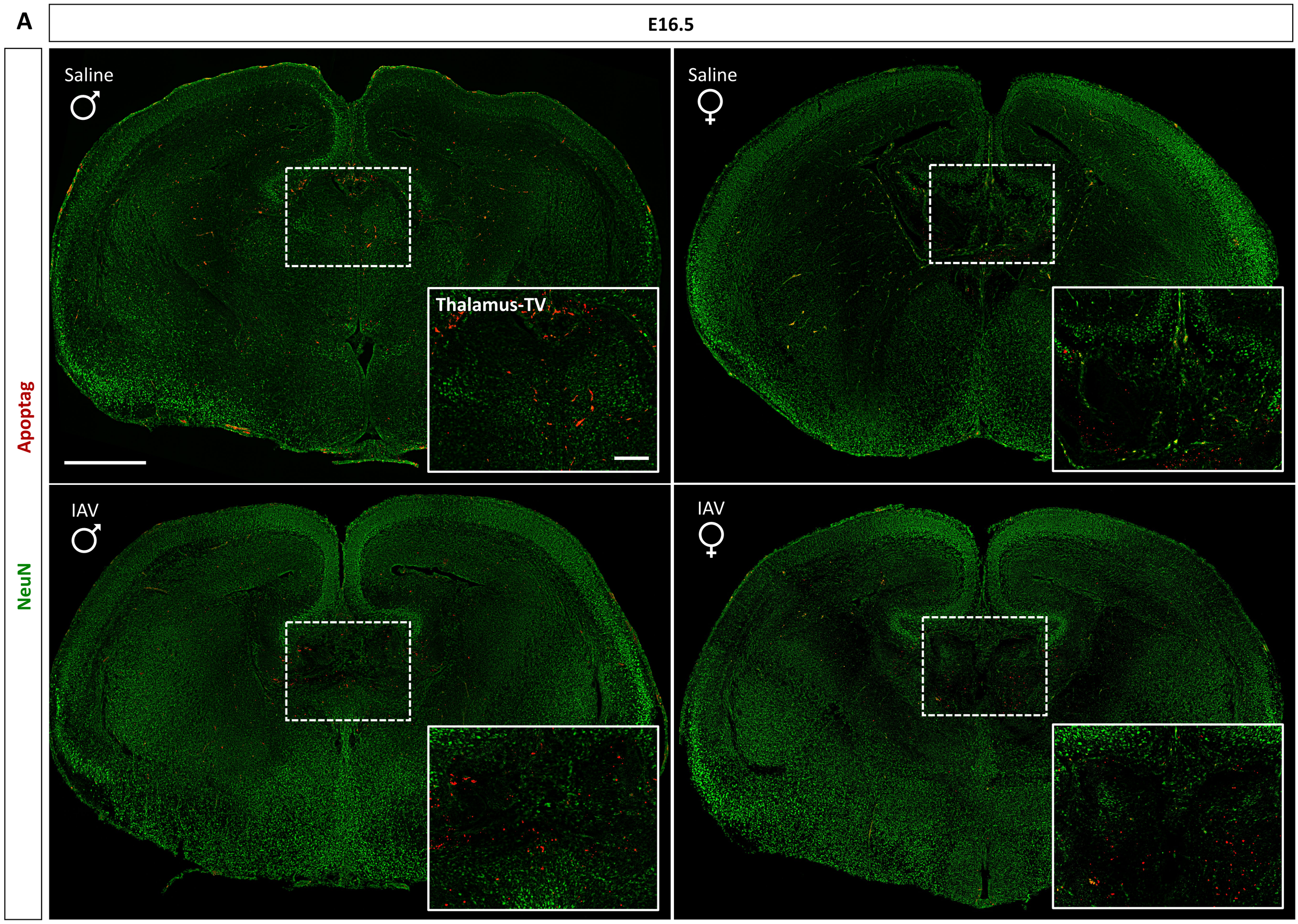

Supplementary Figure S4. Fetal NeuN⁺ neuronal DNA fragmentation is unaffected by maternal flu exposure at E16.5. (A) Representative coronal sections showing NeuN⁺ neurons (green) and ApopTag⁺ apoptotic cells (red) across sex and treatment groups. Insets illustrate the thalamus–third ventricle (Thalamus–TV). In **(B-D)**, NeuN⁺ apoptotic cells in the hemisphere, Thalamus–TV, and SVZ showed no differences between IAV and saline groups in either sex. Likewise, within-treatment sex comparisons revealed no significant differences across all three regions. Data was analyzed using linear mixed-effects models with treatment (saline vs. IAV) and sex (male vs. female) as fixed factors and dam/litter as a random effect. Fixed effects were evaluated using Type III ANOVA with Satterthwaite approximation. No significant effects of treatment, sex, or the treatment × sex interaction were detected. Data represent mean ± SEM; circles represent individual fetuses. n/group: Male = 7-8, Female = 7-8. Scale bars: 500 μm and 100 μm (insets). Thalamus-TV= thalamus-third ventricle.

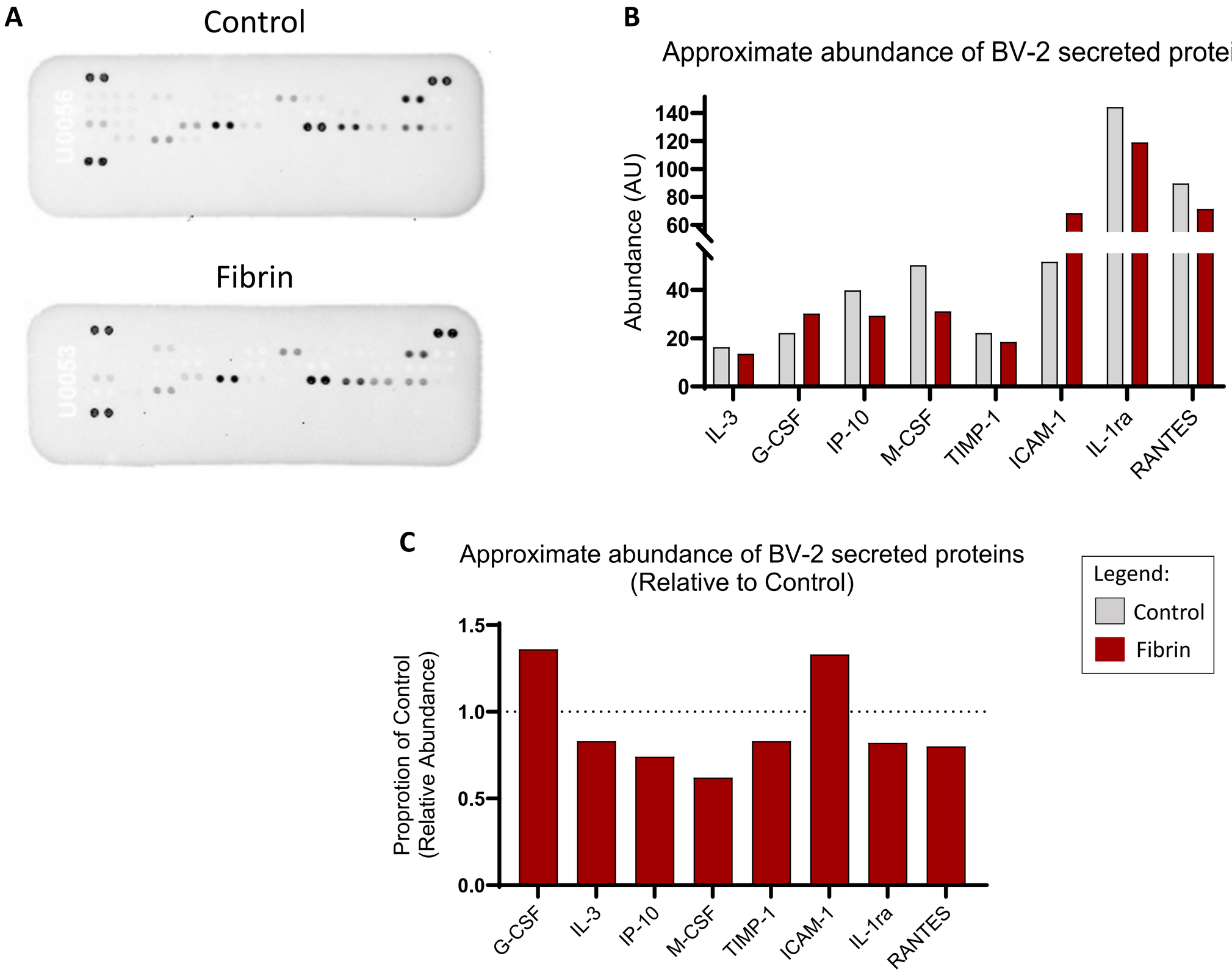

Supplementary Figure S5. Fibrin exposure modestly alters the BV-2 microglial secretome *in vitro*. (**A**) Representative cytokine array membranes showing secreted protein detection in supernatants from control and fibrin-exposed BV-2 cells. (**B**) Approximate abundance of selected BV-2-secreted proteins detected in control and fibrin-treated conditions, expressed as arbitrary units (AU). (**C**) Relative abundance of fibrin-treated samples normalized to control levels for each detected protein. Fibrin exposure modestly altered the abundance of selected secreted proteins, with relative increases in G-CSF and ICAM-1 and lower relative abundance of IL-3, IP-10, M-CSF, TIMP-1, IL-1ra, and RANTES compared with control.

Table S1. List of gene primers for qPCR & Sexing.

Gene	Forward sequence	Reverse sequence
Hprt1	CAAACTTTGCTTTCCCTGGT	TCTGGCCTGTATCCAACACTTC
Hp	GTGGAGCACTTGGTTCGCTA	CCATAGAGCCACCGATGATGC
Crp	TGGCGGGCACTGAACTATAA	CAGGGCTCACAACAGTAGGT
Fga	ACTCGCAACACTAAGAGGGG	GGACATCATCACAGTCTCTCGT
Fgb	GGTGTCTGGGAAAGAGTGTGA	TACGGCTTGATGGAGGTGTC
Fgg	CACGAGACAAGCATTCGGTATT	AGCTGGGCTACCTTCTGTTTTA
X31-np	CAGCCTAATCAGACCAAATG	TACCTGCTTCTCAGTTCAAG
Sry	GTGTCTCAAAGCCTGCTCTTC	CATGTACTGCTAGCAGCTATC
Myog	TTACGTCCATCGTGGACAGCAT	TGGGCTGGGTGTTAGTCTTAT

List of primers used to quantify *Hp*, *Crp*, *Fga*, *Fgb*, *Fgg*, and *X31-np*, with *Hprt1* serving as the housekeeping gene. To assess sex differences, primers for *Sry* were included together with *Myog*, which serves as an internal control gene. X31-np corresponds to the viral nucleoprotein of the X31 influenza strain. *Hp* (Haptoglobin), *Crp* (C-reactive protein), *Fga* (Fibrinogen alpha chain), *Fgb* (Fibrinogen beta chain), *Fgg* (Fibrinogen gamma chain), *Hprt1* (Hypoxanthine-guanine phosphoribosyltransferase 1), *Sry* (Sex-determining Region Y), *Myog* (Myogenin).

Table S2. Litter characteristics of gestating dams at GD16.5.

Outcome	Saline	IAV	p-value
Litter size	8.1 ± 0.6	10.3 ± 0.4	0.02
% Resorptions	8.2 ± 3.5	11.9 ± 2.3	0.45
% Viable	91.79 ± 3.5	88.11 ± 2.3	0.45

Litter size, percentage of viable fetuses, and percentage of reabsorptions per litter were compared between groups using Mann-Whitney tests. Litter size was significantly higher in X31 dams compared with controls (median difference = 2.0; $p = 0.0225$). No statistical differences were detected for % viable fetuses (median difference = –5.55%; $p = 0.4468$) or % resorptions (median difference = 5.55%; $p = 0.4468$). Data are presented as mean ± SEM, with $n = 8$ litters per group. Con = control, IAV = maternal influenza, GD = gestational day.